drones

Article

Exploring Radar Micro-Doppler Signatures for Recognition of Drone Types

Jun Yan [1], Huiping Hu [2], Jiangkun Gong [1,*], Deyong Kong [1,3] and Deren Li [1]

1 State Key Laboratory of Information Engineering in Surveying, Mapping and Remote Sense, Wuhan University, Wuhan 430072, China; yanjun_pla@whu.edu.cn (J.Y.)
2 Wuhan Geomatics Institute, Wuhan 430022, China
3 School of Information and Communication Engineering, Hubei University of Economics, Wuhan 430205, China
* Correspondence: gjk@whu.edu.cn; Tel.: +86-027-68778527

Abstract: In this study, we examine the use of micro-Doppler signals produced by different blades (i.e., puller and lifting blades) to aid in radar-based target recognition of small drones. We categorize small drones into three types based on their blade types: fixed-wing drones with only puller blades, multi-rotor drones with only lifting blades, and hybrid vertical take-off and landing (VTOL) fixed-wing drones with both lifting and puller blades. We quantify the radar signatures of the three drones using statistical measures, such as signal-to-noise ratio (SNR), signal-to-clutter ratio (SCR), Doppler speed, Doppler frequency difference (DFD), and Doppler magnitude ratio (DMR). Our findings show that the micro-Doppler signals of lifting blades in all three drone types were stronger than those of puller blades. Specifically, the DFD and DMR values of pusher blades were below 100 Hz and 0.3, respectively, which were much smaller than the 200 Hz and 0.8 values for lifting blades. The micro-Doppler signals of the puller blades were weaker and more stable than those of the lifting blades. Our study demonstrates the potential of using micro-Doppler signatures modulated by different blades for improving drone detection and the identification of drone types by drone detection radar.

Keywords: automatic target recognition (ATR); drone blades; drone type classification; micro-Doppler

Citation: Yan, J.; Hu, H.; Gong, J.; Kong, D.; Li, D. Exploring Radar Micro-Doppler Signatures for Recognition of Drone Types. *Drones* **2023**, *7*, 280. https://doi.org/10.3390/drones7040280

Academic Editors: Zain Anwar Ali and Quanmin Zhu

Received: 12 April 2023
Revised: 18 April 2023
Accepted: 20 April 2023
Published: 21 April 2023

1. Introduction

Drones, also known as small unmanned aerial vehicles (UAVs), have revolutionized the modern world. These devices have proven to be valuable tools in a variety of civil applications, such as aerial photography, agriculture, remote sensing, transportation, and recreation [1–4]. At the same time, military drones have challenged the rules of modern warfare, as demonstrated by their victories in conflicts such as the Nagorno-Karabakh and Ukraine wars [5–8]. With the rapid growth in drone usage, there is an increasing demand for drone detection systems.

Radar sensors have emerged as the most effective tools for detecting and tracking drones, given their long-range detection capabilities, efficiency, large visual angle, high update rates, and weather independence [9,10]. However, detecting and classifying drones using radar presents unique challenges due to their small size, low radar cross-section, and variable flight patterns [11]. Additionally, most drones belong to Group 1 (Table 1), as defined by the U.S. Department of Defense, requiring rotating blades to fly in the sky [12]. As a result, researchers must develop sophisticated techniques for detecting and tracking drones, particularly those that are not quad-rotor drones.

Drones are known to produce micro-Doppler shifts in radar echoes due to the modulation of incident radar waves by their rotating blades [13]. These shifts are unique radar signatures that can aid in the detection and classification of drones from other clutter, such as birds and humans [14–20]. Drones can be classified into three types based on the relative direction between the rotating plane of blades and the ground plane. The first type consists of drones with only lifting blades, such as single-rotor helicopter drones, quad-rotor drones, and other multi-rotor drones. The second type has only puller (or pusher) blades, such as fixed-wing drones, where the puller blades rotate perpendicular to the ground plane and provide propulsive force for forward flight, while the lifting force comes from air wings. The third type is the hybrid drone with both puller blades and lifting blades, providing the advantages of fixed-wing drones and the ability to hover, making them a new category of hybrid vertical take-off and landing (VTOL) fixed-wing drones.

Table 1. Drone classification according to the US Department of Defense (DoD) [1,2].

Category	Size	Maximum Gross Takeoff Weight (Pounds)	Normal Operating Altitude (ft)	Airspeed (Knots)
Group 1	Small	0–20	<1200 Above Ground Level (AGL)	<100
Group 2	Medium	21–55	<3500 AGL	<250
Group 3	Large	<1320	<18,000 Mean Sea Level (MSL)	
Group 4	Larger	<1320		Any airspeed
Group 5	Largest	>1320	>18,000 MSL	Any airspeed

[1] Source: "Eyes of the Army", U.S. Army Roadmap for UAS 2010–2035. https://home.army.mil/rucker/index.php, accessed on 19 April 2023. [2] If the drone has even one characteristic of the next level, it is classified in that level.

This paper investigates the micro-Doppler shifts produced by the following three drone types: a fixed-wing drone, a quad-rotor drone, and a hybrid VTOL drone. The theoretical scattering models of the two types of blades, the lifting blade, and the puller one are analyzed in Section 2, and the micro-Doppler shifts are compared with the body Doppler. Section 3 presents the detection results of radar signals from the three drones, and the differences in micro-Doppler shifts in their radar echoes are compared. Section 4 discusses the applications of the different micro-Doppler shifts of the three drones. Finally, in Section 5, we conclude that micro-Doppler shifts can be used to classify drone types.

The following are the key novelties of our study:

(1) We have categorized small drones based on blade types, including multi-rotor drones with only lifting blades, fixed-wing drones with only puller blades, and hybrid VTOL drones with both lifting and puller blades.

(2) We have developed parameters, such as the Doppler frequency difference (DFD) and the Doppler magnitude ratio (DMR), to describe the micro-Doppler differences produced by the two types of blades.

(3) Our investigation reveals that puller blades generate weaker and more stable micro-Doppler signals compared to lifting blades, which can facilitate the radar-based recognition of drone types.

2. Materials and Methods

2.1. Scattering Model

The Doppler spectrum of drones consists of three components: the body Doppler, the micro-Doppler, and the clutter Doppler. To illustrate this, consider the geometry shown in Figure 1, which depicts the radar, the drone body, and a rotating rotor blade. Let O be the center of the drone body and P be the center of the blade, which rotates from P_0 to P_t. The radar's range is denoted as R, the blade length is L, the azimuth angle is α, and the elevation angle is β. The phase angle of the blade's rotation is φ_t, which is a function of the rotating speed ω. The radar wavelength is represented by λ. The Doppler shifts can be computed as follows:

$$\overline{f_d(t)} = \overline{f_{bd}} + \overline{f_{md}(t)} + \overline{f_{cd}(t)} \tag{1}$$

where $\overline{f_{bd}}$ = the body Doppler vector, $\overline{f_{md}(t)}$ = the micro-Doppler vector, and $\overline{f_{cd}(t)}$ = the clutter Doppler vector, which are caused by the clutter. However, since the clutter Doppler has small magnitudes and low shifts, it can be neglected, and the main components are the body Doppler and the micro-Doppler. Assuming that the drone's speed is V_b, the body Doppler components due to the Doppler effect can be given as:

$$\overline{f_{bd}} = -\frac{2V_b}{\lambda} \tag{2}$$

Since the lifting blade rotates almost parallel to the ground plane during cruise flight, the micro-Doppler shift can be approximated by the radial component of the blade velocity projected onto the radar line-of-sight. This is given by:

$$\overline{f_{md}(t)_{\parallel}} = \frac{L}{\lambda}\omega cos\beta \ \cos(\omega t) + \overline{f_{bd}} \tag{3}$$

However, since the puller blade rotates in a direction perpendicular to the ground plane, its micro-Doppler can be calculated using the following equation:

$$\overline{f_{md}(t)_{\perp}} = \frac{L}{\lambda}\omega cos\alpha \ cos\beta \ \cos(\omega t) + \overline{f_{bd}} \tag{4}$$

The magnitude of the micro-Doppler can be obtained through the inverse Fourier transformation. Comparing Equations (3) and (4), it can be inferred that the micro-Doppler shift and magnitude of a puller blade are lower than those of a lifting blade, despite having the same physical parameters.

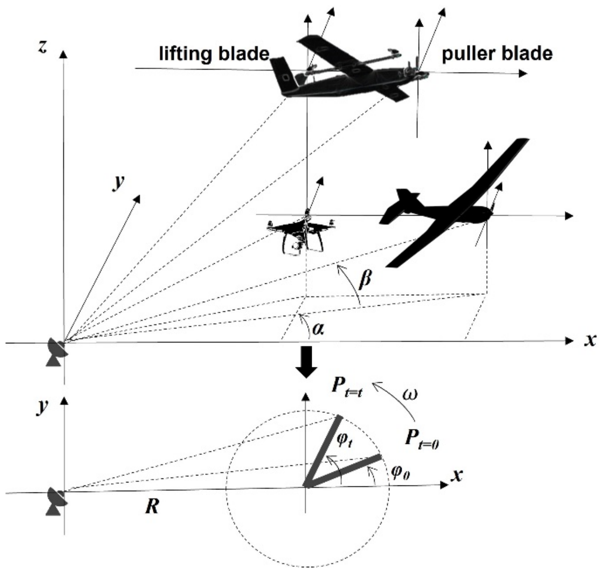

Figure 1. The geometry of the radar and the rotating rotor blades of different types of drones.

Micro-Doppler signatures are not solely represented by the Doppler shifts given in Equations (3) and (4). Typically, micro-Doppler signatures are characterized as sinusoidal modulation associated with the rotating rate, ω, as expressed in Equations (3) and (4). This modulation appears as a frequency trajectory on a 2D joint time–frequency image, which can be generated using a short-time Fourier transformation (STFT) or other transformations [21–23]. Additionally, the micro-Doppler reaches its maximum when the incident wave is perpendicular to the narrow face of the blade (i.e., $\varphi_t = 0$). At this point in time, strong reflection signals related to the blade are present in the time series of the drone's radar echoes, which is commonly known as the "blade flash" signal. These signals also appear as jet engine modulation (JEM)-like micro-Doppler frequencies in the spectrum.

2.2. Metrics

Here, we employ the JEM method to analyze the micro-Dopplers of various drone types. The micro-Doppler signatures are characterized by four parameters. The first parameter is the signal-to-noise ratio (SNR) of the radar signals, denoted by P_{SNR}, which is calculated as follows:

$$P_{SNR}(\text{dB}) = 10 \log 10(\frac{S}{N}) \tag{5}$$

where S = the magnitude of the radar signals from the target and N = the magnitude of the noise level. The second parameter is the maximum signal-to-clutter ratio (SCR), given by

$$P_{SCR}(\text{dB}) = 10 \log 10(\frac{F_{max}}{F_{mean}}) \tag{6}$$

where F_{max} = the maximum magnitude of the bulk Doppler in the spectrum and F_{mean} = the mean magnitude of the Dopplers in the spectrum. The third parameter is the Doppler frequency difference (DFD) between the body Doppler and the nearest micro-Doppler, represented by

$$P_{DFD} = \left| |\overline{f_{bd}}| - |\overline{f_{md0}}| \right| \tag{7}$$

where $|\overline{f_{bd}}|$ = the module of the body Doppler and $|\overline{f_{md0}}|$ = the module of the nearest micro-Doppler. Finally, the fourth one is the Doppler magnitude ratio (DMR) of the nearest micro-Doppler to the body Doppler, given by

$$P_{DMR} = \frac{A_{md0}}{A_{bd}} \tag{8}$$

where A_{bd} = the magnitude of the body Doppler and A_{md0} = the magnitude of the nearest micro-Doppler.

2.3. Experiments

The radar system utilized in this study is an X-band pulse-Doppler phased array radar with a narrow bandwidth, providing a range resolution of approximately 12 m. The radar operates with a coherent pulse interval (CPI) of approximately 20 milliseconds and a pulse repetition frequency (PRF) of approximately 5 kHz. Each CPI consists of 96 sample points, but we use zero padding to increase it to 256 points. As a result, the mathematical Doppler frequency resolution is around 19.5 Hz. Equipped with an active electronically scanned antenna (AESA), the radar system is mounted on a rotating table to achieve 360° coverage in azimuth scans.

With a detection response time (DRT) of several milliseconds, the radar system can present detection and recognition results with graphic icons in the real-time mode, which label the recognition results and the rotating motion of the scanning beam, as illustrated in Figure 2. The icons are associated with tracking numbers for the detected objects. In the example shown in Figure 2, objects detected in a coastal area include ships, birds, drones, and others, with three drones serving as cooperative targets. The Albatross1 is a homemade fixed-wing drone, the DJI Phantom 4 is a quad-copter drone, and the TX25A is a large VTOL drone. Table 2 presents several parameters of the drones tested, while Figure 2 provides visual representations of the drones. During the experiments, the drones followed pre-planned flight paths guided by GPS coordinates on a map. Typically, the drones flew either directly away from or towards the radar in a straight line. The radar, operating in tracking mode, recorded the radar signals emitted by the drones during these flights.

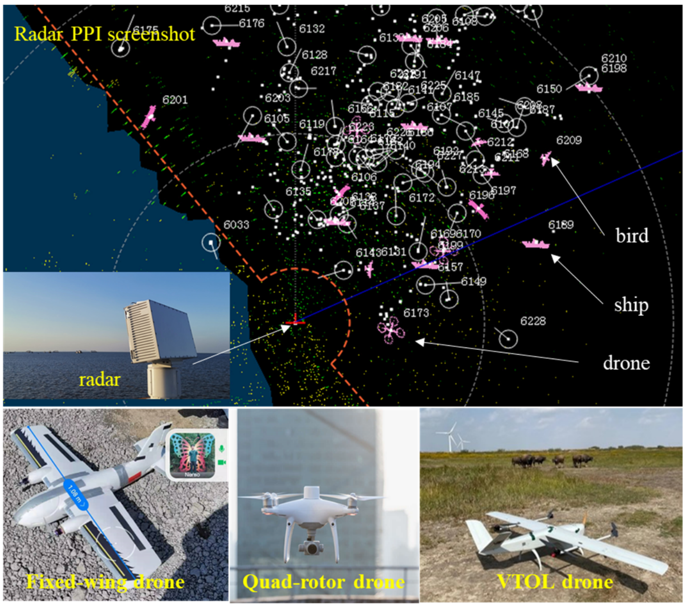

Figure 2. The photos of the radar and drones.

Table 2. Drone parameters.

Drone Type		Fixed-Wing Drone	Quad-Rotor Drone	VTOL Drone
Model		Albatross1	Phantom 4	TX25A
Manufacturer		Homemade	DJI Inc.	Harryskydream Inc.
Flight weight (kg)		0.3	1.38	26
Body size (cm)		80	40	197
Wingspan (cm)		108	40	360
Cruise speed (m/s)		10	15	25
Blades	lifting	0	4	4
	puller	1	0	1
Blade length(cm)		10	20	30
Aero-frame materials		EPP (Expanded polypropylene)	PC (Polycarbonate)	FRP (Fiber-reinforce plastic)

3. Results

There are micro-Doppler signals present in the spectra of the three drones. Figure 3 shows a comparison between the raw time series and spectra of the fixed-wing drone, quad-rotor drone, and VTOL drone. The sample time in one CPI is approximately 20 ms, and the Dopplers in the spectra are given as Doppler velocities. The values on the vertical axis are normalized. Typically, the Doppler of background clutter is around 0 Hz, but the target's Doppler can suppress the clutter. 'High-speed' data indicate that the drone was flying at a high velocity, and 'low-speed' data represent the drone flying at a low velocity. The body Dopplers (i.e., the bulk Dopplers) in the spectrum indicate the flying speeds of drones, which are −19.24 m/s and 1.68 m/s in Figure 3a, −7.84 m/s and 2.52 m/s in Figure 3b, and −12.04 m/s and 0.28 m/s in Figure 3c.

In Figure 3a, the micro-Dopplers (−10.92 m/s, 2.52 m/s) of the puller blades of the fixed-wing drone seem to stay close to the neighbors of the body Dopplers, with very low magnitudes. However, the micro-Dopplers (−5.88 m/s, 4.76 m/s) of the quad-rotor drone's lifting blades in Figure 3b are strong enough to be comparable to the body Dopplers. The micro-Dopplers of the VTOL drone in Figure 3c are also distributed in the same pattern, where the puller ones (10.64 m/s, 5.04 m/s) have small magnitudes but the lifting ones (−14 m/s, 3.92 m/s) have larger magnitudes. Regardless of the number and magnitude of micro-Dopplers, they are significant. Furthermore, a drone flying at a low speed may have its body Doppler cluttered by the background clutter around 0, but its micro-Doppler shifts can stand out. Therefore, the micro-Doppler may be helpful in the radar detection of drones, especially hovering drones.

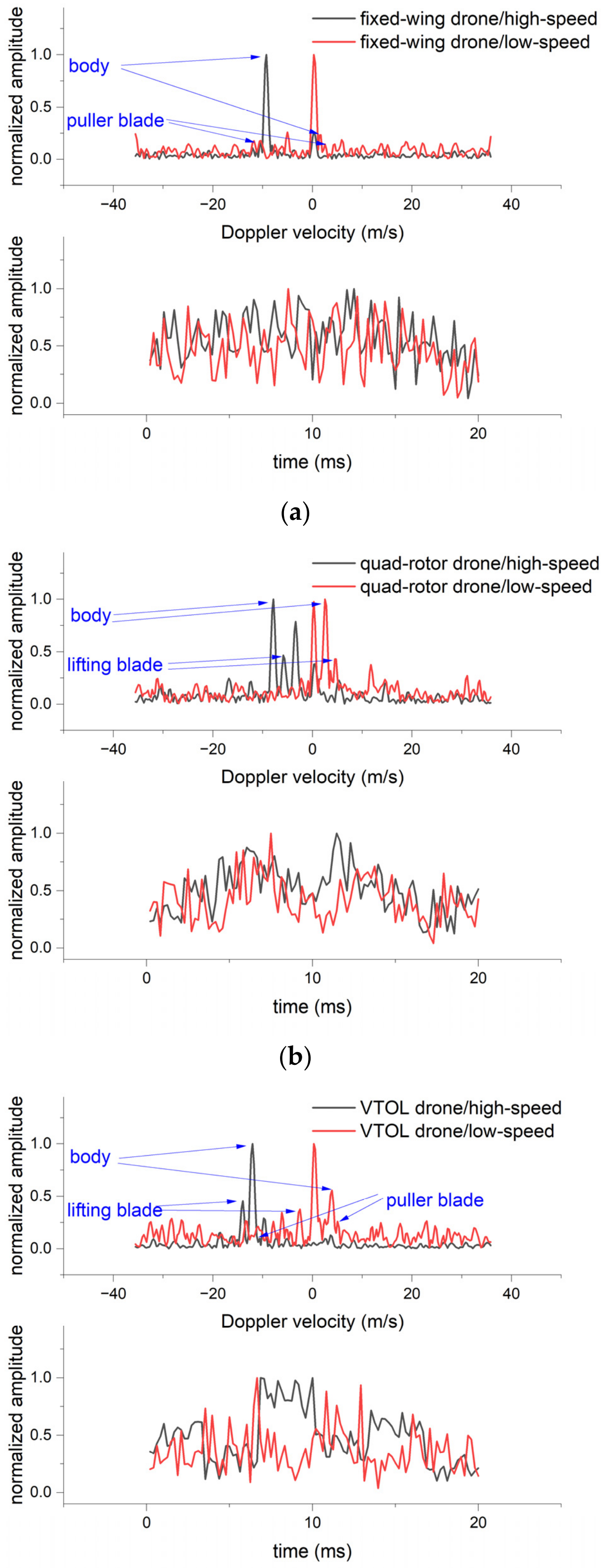

(a)

(b)

(c)

Figure 3. Radar echoes and spectrum of drones. (**a**) The fixed-wing drone, (**b**) the quad-rotor drone, (**c**) the VTOL drone.

The tracking results of micro-Doppler signatures using Equations (5)–(8) indicate that the distribution patterns of micro-Dopplers shown in Figure 3 are not rare occurrences, but rather common ones. Figure 4 compares the three drones' Doppler frequency difference (DFD) and the Doppler magnitude ratio (DMR). For the fixed-wing drone's puller blade, most DFD values are about 100 Hz, and the DMR values are less than 0.2, as shown in Figure 4a. However, the DFD and DMR values for the quad-rotor drone's lifting blades are higher, around 200 Hz and 0.5, respectively, as seen in Figure 4b. The comparison of micro-Dopplers in Figure 4c is even more apparent. The number, DFD, and DMR of the puller blades are much smaller than those of the lifting blades of the VTOL drone.

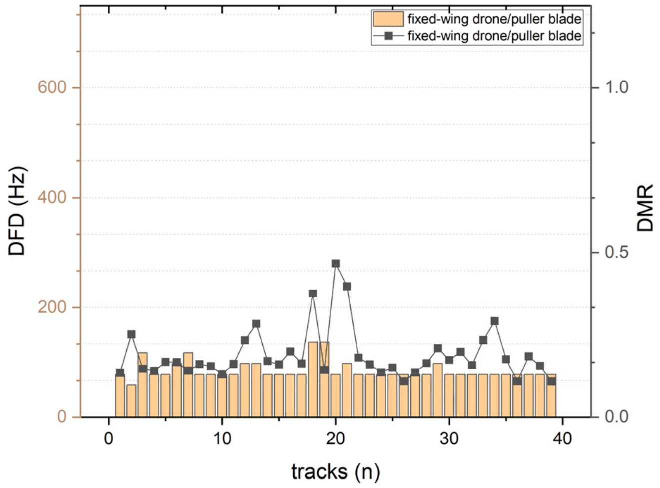

(**a**)

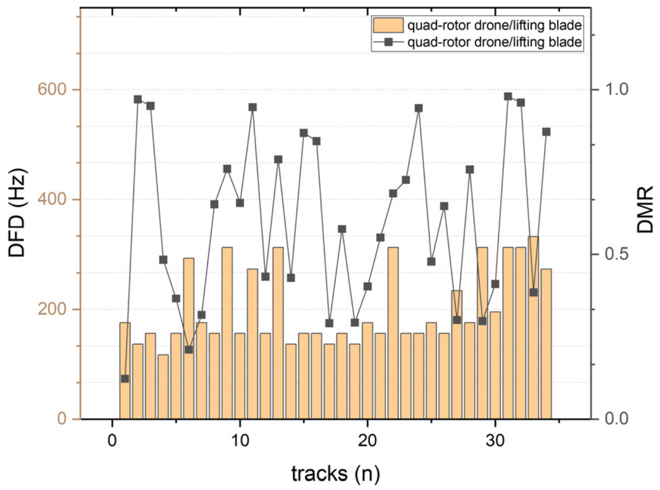

(**b**)

Figure 4. *Cont.*

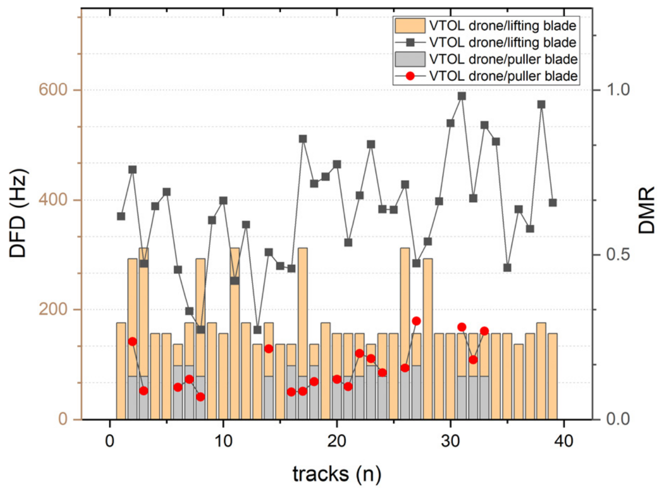

(**c**)

Figure 4. Body doppler and micro-Doppler data of drones. (**a**) The fixed-wing drone, (**b**) the quad-rotor drone, (**c**) the VTOL drone.

The statistical results presented in Table 3 (based on data in Figure 4) show that the micro-Doppler signals of lifting blades are generally stronger than those of puller blades, regardless of the drone type. The tracking distances from the radar for all three drones were similar, around 10 km. However, the VTOL drone had a higher average speed (about 12.0 m/s) compared to the fixed-wing drone (about 6.4 m/s) and the quad-rotor drone (about 4.9 m/s).

Table 3. Comparison of detection performances [1].

Object		Fixed-Wing Drone	Quad-Rotor Drone	VTOL Drone	
Tracking distance (km)		11~12	10~11	9~13	
Velocity (m/s)	Mean	6.46	4.94	12.04	
	Range	10.92	6.16	6.16	
SNR (dB)	Mean	2.27	1.20	4.07	
	Range	6.4	9.23	11.21	
SCR (dB)	Mean	13.79	10.86	12.79	
	Range	7.84	5.51	8.73	
Blade		Puller blade	Lifting blade	Puller blade	Lifting blade
DFD (Hz)	Mean	85.13	202.76	85.31	182.78
	Range	78.12	214.83	19.53	175.77
DMR	Mean	0.18	0.59	0.15	0.63
	Range	0.35	0.85	0.23	0.71

[1] It is important to note that the radar was operating in tracking mode. As a result, we are specifically interested in assessing the detection capability of micro-Doppler signals from drones in this context. This evaluation prioritizes the performance of micro-Doppler signals over traditional metrics, such as range, detection probability, and false alarm rate.

In Table 3, "Mean" represents the average value of each parameter and "Range" indicates the difference between the minimum and maximum values. The puller Doppler signals generally have lower magnitudes and slower shifts than lifting Doppler signals, regardless of the drone type. For example, the mean DFD and DMR values of the fixed-wing drone's puller Doppler signals were 78.12 Hz and 0.18, respectively, which were smaller than those of the VTOL drone's puller Doppler signals (mean DFD: 19.53 Hz; mean DMR: 0.15) and much smaller than those of the quad-rotor drone's lifting Doppler signals (mean DFD: 214.83 Hz; mean DMR: 0.59) and the VTOL drone's lifting Doppler signals (mean DFD: 182.78 Hz; mean DMR: 0.63). The "Range" values for the puller Doppler signals (0.35

for the fixed-wing drone and 0.23 for the VTOL drone) were generally lower than those for the lifting Doppler signals (0.85 for the quad-rotor drone and 0.71 for the VTOL drone). The micro-Dopplers produced by the puller blades are weaker but more stable than the lifting blades, which is related to the radial component seen by the radar, as explained in Figure 1, and Table 3.

4. Discussion

Micro-Dopplers produced by rotating blades can serve as more effective signatures for radar automatic target recognition (ATR) than traditional measures such as radar cross-section (RCS) and speeds. Figure 5 depicts the tracking speeds, signal-to-noise ratio (SNR), and signal-to-clutter ratio (SCR) values of the three drones. Table 3 presents the statistical results of these values for the drones, which were all tracked in a similar detection range of 10 km.

According to the mean speeds, the VTOL drone was the fastest, followed by the fixed-wing drone and the quad-rotor drone. However, all three types of drones are capable of flying at a range of speeds, from 0.28 m/s to 11.2 m/s for the fixed-wing drone, 1.68 m/s to 7.84 m/s for the quad-rotor drone, and 9.24 m/s to 15.4 m/s for the VTOL drone. Additionally, their SNR, SCR values, and flying speeds overlap in Figure 5, suggesting that these may not be reliable or robust signatures for radar ATR applications.

Micro-Dopplers have been shown to be more effective signatures for identifying radar signals of drones compared to measures such as speed, signal-to-noise ratio (SNR), and signal-to-clutter ratio (SCR). Figure 6 provides histograms of the detected values of the different drones in Figure 5, including the speed, the SNR, the SCR, the DFD, and the DMR values. Since the VTOL drone has a larger size and faster speeds than the fixed-wing drone and the quad-rotor drone, as shown in Table 2, the measured speed, SNR, and SCR values of the VTOL drone are higher. However, some of them are also mixed. Essentially, speed, SNR, and SCR are the features providing a general characteristic (i.e., a 'point' feature) of a drone, but they do not provide details (i.e., a 'structure' feature) about the target. Detailed intelligence is extracted using the micro-Doppler signals.

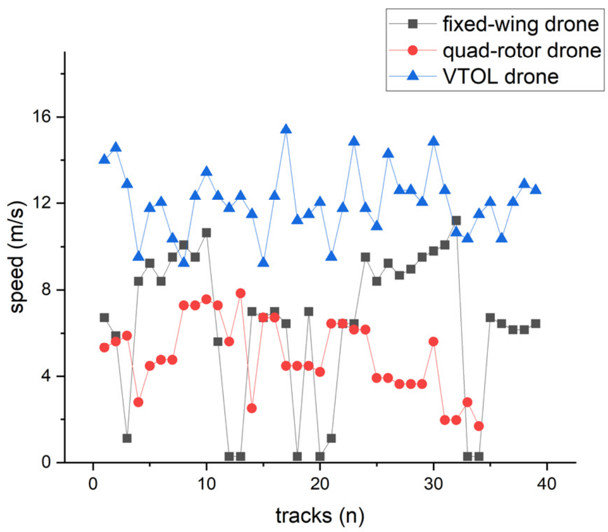

(**a**)

Figure 5. *Cont.*

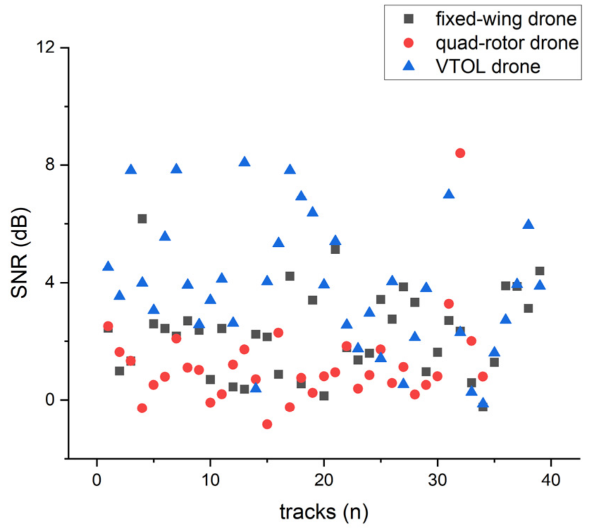

(**b**)

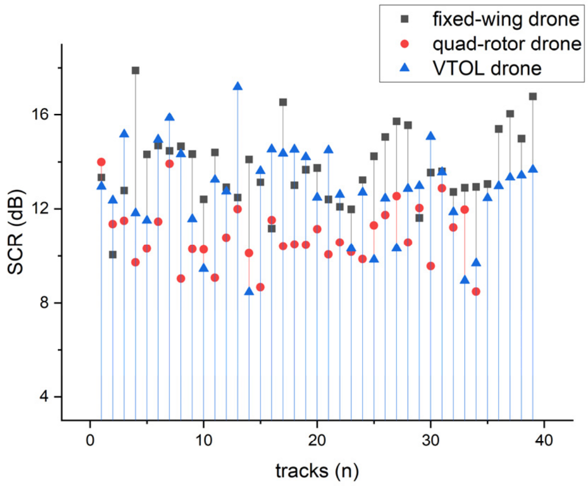

(**c**)

Figure 5. Tracking speeds, SNR, and SCR values of drones. (**a**) The fixed-wing drone, (**b**) the quad-rotor drone, (**c**) the VTOL drone.

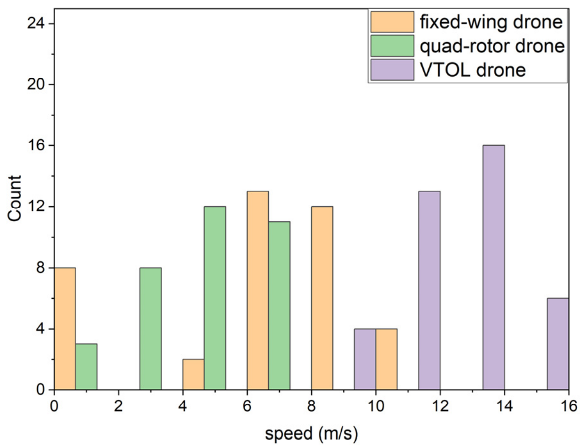

(**a**)

Figure 6. *Cont.*

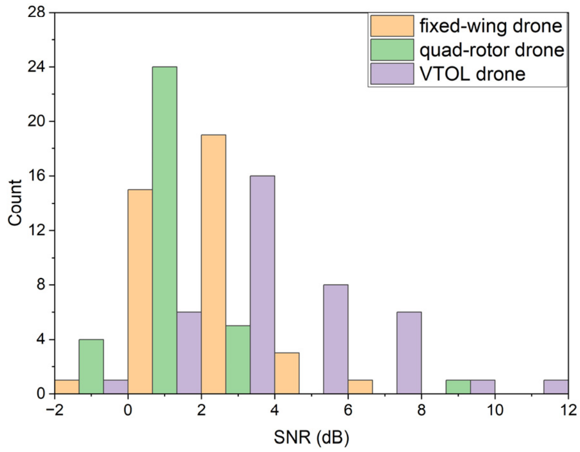

(**b**)

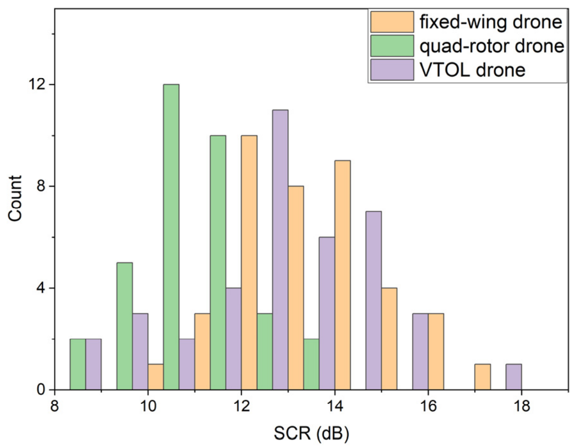

(**c**)

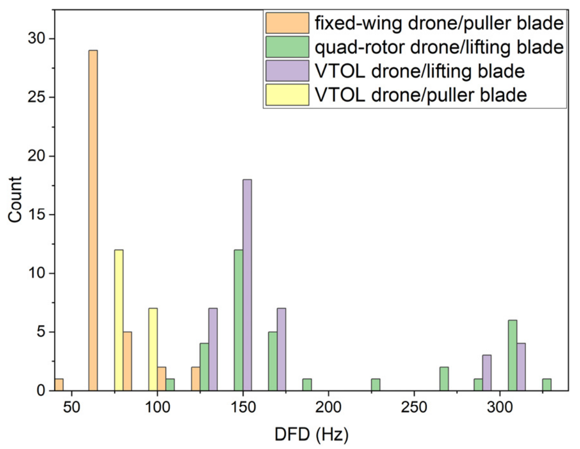

(**d**)

Figure 6. *Cont.*

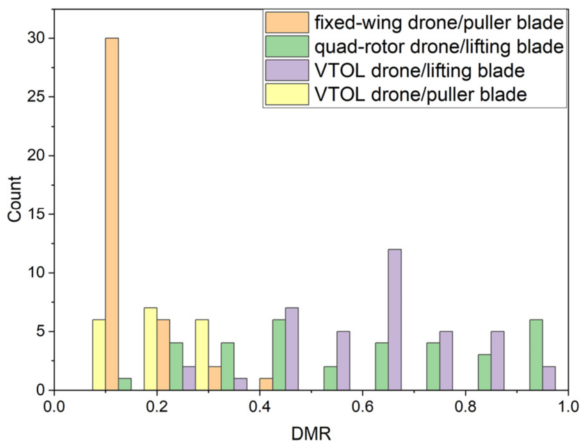

(**e**)

Figure 6. The histograms of detection values of drones. (**a**) The speed values, (**b**) the SNR values, (**c**) the SCR values, (**d**) the DFD values, (**e**) the DMR values.

All three types of drones produce micro-Dopplers in their spectra, and the presence or absence of such micro-Doppler shifts (JEM) can help differentiate drone signals from clutter such as birds or people. Secondly, differences in the micro-Doppler patterns between the drones, such as oscillation frequency deviation (DFD) and Doppler modulation ratio (DMR), can be used to identify the blade types and then recognize the drone types. For example, stable, narrow (less than 100 Hz), and weak (less than 0.5) DFD and DMR in a drone's micro-Doppler spectrum may indicate the presence of a puller blade, whereas a larger DFD (200 Hz or greater) and DMR (greater than 0.5) may suggest a lifting blade. A drone with only lifting blades is likely to be a quad-rotor drone, while a drone with only puller blades is likely a fixed-wing drone. Therefore, a drone with both lifting and puller blades is classified as a VTOL drone.

Figure 7 illustrates a flowchart of an ATR algorithm that considers micro-Doppler signatures to distinguish small drones from other aircraft types. However, in a real environment, other aircraft types, such as helicopters and jets, can also produce micro-Doppler signals similar to small drones. Therefore, to improve the accuracy of the ATR algorithm, additional features such as kinematic characteristics (e.g., speed) and amplitude signatures (e.g., SNR, SCR) can be combined with micro-Doppler signatures. For example, if an airborne target is detected with a speed over 200 km/h and an RCS value of 100 m^2, it can be confidently classified as a non-small drone. Including these additional features can expedite the recognition process and increase recognition accuracy. Nonetheless, micro-Doppler signatures corresponding to different blade types (i.e., lifting and puller blades) remain crucial for accurate ATR of small drones.

Recognizing drone types holds significance in two areas: (1) unmanned aircraft traffic management (UTM) systems in civil applications; (2) the counter-drone applications for military clients. The UTM concept aims to manage drones flying at low altitudes around/at airports [24]. Different types of drones have different flying speeds and heights, making it necessary to identify them to monitor and manage airspace. Once the UTM system recognizes the drone types, it can plan flight routes for cooperative drones [25,26] and process uncooperative drones. Note that radar may become the vital sensor in future UTM systems as it can provide active detection and sensing intelligence. Thus, radar with automatic target recognition (ATR) of drone types is necessary for UTM clients. Furthermore, the recent wars in Nagorno-Karabakh and Ukraine indicate that different types of drones can play distinct roles in battles. Several countermeasures such as electronic jamming, laser weapons, and kinetic weapons can impact a drone in flight and disable/damage drones [9,10]. Therefore, counter-drone systems must be adjusted to process different threats from different types of drones. For instance, it may not be an economical solution to use kinetic systems to disable small quad-rotor drones such as 'DJI Phantom 4'. Similarly, it may be futile to utilize laser weapons to disable a large fixed-wing drone such as 'Bayraktar TB2' or use electronic jamming to disable a suicide drone such as 'Switchblade 600'. The precondition for countermeasures is the recognition of drone types using radar and other sensors such as EO/IR equipment.

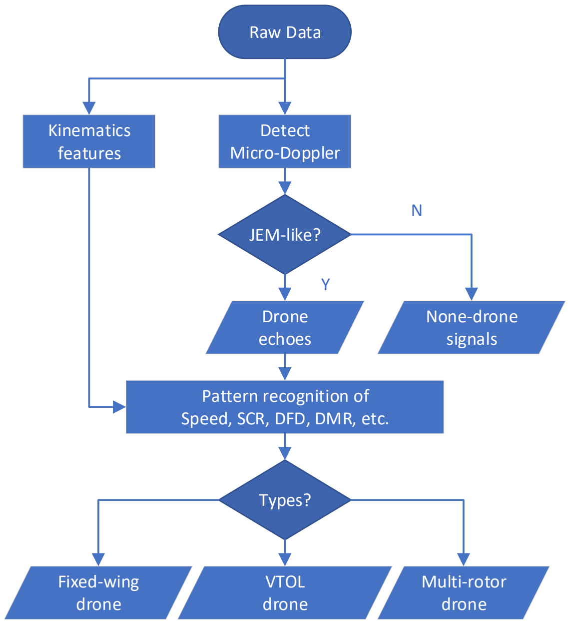

Figure 7. The block diagram of the ATR algorithm using micro-Doppler to recognize drone types.

5. Conclusions

Group 1 includes many types of drones that require detection and classification by drone detection radar. Drones can be categorized based on blade types, including lifting blades and puller (or pusher) blades, into three types: fixed-wing drones with only puller blades, multi-rotor drones with only lifting blades, and VTOL drones with both lifting and puller blades. This study compared the radar signatures of these three drone types using an X-band pulse-Doppler radar. The results indicated that all drone radar signals had micro-Dopplers modulated by the rotating blades, but the micro-Doppler of the puller blades was weaker than that of the lifting blades. Statistical data showed that the Doppler frequency difference (DFD) and Doppler magnitude ratio (DMR) of pusher blades were below 100 Hz and 0.3, respectively, which were much smaller than the 200 Hz and 0.8 values for lifting blades. These micro-Doppler signatures can be used to recognize blade types and enable radar automatic target recognition (ATR) of the three drone types. The fixed-wing drone has only puller blades, while the quad-rotor drone has only lifting blades. The VTOL drone, on the other hand, has both lifting and puller blades. Therefore, recognizing the blade types can help classify the drone type, which is useful for ATR applications.

Author Contributions: Conceptualization, J.Y. and J.G.; formal analysis, J.Y.; funding acquisition, D.K.; investigation, J.G.; supervision D.L.; visualization, H.H.; writing—original draft, J.G.; writing—review and editing, H.H. All authors have read and agreed to the published version of the manuscript.

Funding: This research received some support from the Natural Science Foundation of Hubei Providence via General Program-2021CFB309.

Institutional Review Board Statement: Not applicable.

Informed Consent Statement: Not applicable.

Data Availability Statement: Some of the data presented in this study may be available on request from the corresponding author. The data are not publicly available due to the internal restrictions of the research group.

Acknowledgments: We appreciate both the testers who aided in the collection of the data, and we also want to thank the authors whose photographs are reproduced in this study.

Conflicts of Interest: The authors declare that they have no conflicts of interest.

References

1. Milas, A.S.; Cracknell, A.P.; Warner, T.A. Drones—The third generation source of remote sensing data. *Int. J. Remote Sens.* **2018**, *39*, 7125–7137. [CrossRef]
2. Sun, Z.; Wang, X.; Wang, Z.; Yang, L.; Xie, Y.; Huang, Y. UAVs as Remote Sensing Platforms in Plant Ecology: Review of Applications and Challenges. *J. Plant Ecol.* **2021**, *14*, 1003–1023. [CrossRef]
3. Petrovski, A.; Bogatinov, D.; Radovanović, M. *Application of Drones in Crises Management Supported Mobile Applications and C4IRS Systems*; Springer International Publishing: New York, NY, USA, 2023; pp. 321–334. ISBN 978-3-031-26753-6.
4. Yang, B.; Li, J. A Hierarchical Approach for Refining Point Cloud Quality of a Low Cost UAV LiDAR System in the Urban Environment. *ISPRS J. Photogramm. Remote Sens.* **2022**, *183*, 403–421. [CrossRef]
5. Semercioğlu, H. The New Balance of Power in the Southern Caucasus in the Context of the Nagorno-Karabakh Conflict in 2020. *RS Res. Stud. Anatolia J.* **2021**, *4*, 49–60.
6. Kunertova, D. The War in Ukraine Shows the Game-Changing Effect of Drones Depends on the Game. *Bull. At. Sci.* **2023**, *79*, 95–102. [CrossRef]
7. Ilić, D.; Tomašević, V. The impact of the Nagorno-Karabakh conflict in 2020 on the perception of combat drones. *Serb. J. Eng. Manag.* **2021**, *6*, 9–21. [CrossRef]
8. Pong, B. The Art of Drone Warfare. *J. War Cult. Stud.* **2022**, *15*, 377–387. [CrossRef]
9. Markarian, G.; Staniforth, A. *Countermeasures for Aerial Drones*; Artech: London, UK; Norwood, MA, USA, 2020.
10. Clemente, C.; Fioranelli, F.; Colone, F.; Li, G. *Radar Countermeasures for Unmanned Aerial Vehicles*; IET: London, UK, 2021; ISBN 9781839531903.
11. Wellig, P.; Speirs, P.; Schuepbach, C.; Oechslin, R.; Renker, M.; Boeniger, U.; Pratisto, H. Radar Systems and Challenges for C-UAV. In Proceedings of the International Radar Symposium 2018, Nanjing, China, 17–19 October 2018; Volume 2018, pp. 1–8.
12. U.S. Army Unmanned Aircraft Systems Center of Excellence. Eyes of the Army. In *U.S. Army Unmanned Aircraft Systems Roadmap 2010–2035*; U.S. Army Unmanned Aircraft Systems Center of Excellence: Fort Rucker, AL, USA, 2010.
13. Hanif, A.; Muaz, M.; Hasan, A.; Adeel, M. Micro-Doppler Based Target Recognition with Radars: A Review. *IEEE Sens. J.* **2022**, *22*, 2948–2961. [CrossRef]
14. Rudys, S.; Ragulis, P.; Laučys, A.; Bručas, D.; Pomarnacki, R.; Plonis, D. Investigation of UAV Detection by Different Solid-State Marine Radars. *Electronics* **2022**, *11*, 2502. [CrossRef]
15. Molchanov, P.; Harmanny, R.I.A.; De Wit, J.J.M.; Egiazarian, K.; Astola, J. Classification of Small UAVs and Birds by Micro-Doppler Signatures. *Int. J. Microw. Wirel. Technol.* **2014**, *6*, 435–444. [CrossRef]
16. Molchanov, P.; Egiazarian, K.; Astola, J.; Harmanny, R.I.A.; de Wit, J.J.M. Classification of small UAVs and birds by micro-Doppler signatures. In Proceedings of the 2013 European Radar Conference, Nuremberg, Germany, 9–11 October 2013; pp. 172–175.
17. Palamà, R.; Fioranelli, F.; Ritchie, M.; Inggs, M.; Lewis, S.; Griffiths, H. Measurements and discrimination of drones and birds with a multi-frequency multistatic radar system. *IET Radar Sonar Navig.* **2021**, *15*, 841–852. [CrossRef]
18. Dale, H.; Jahangir, M.; Baker, C.J.; Antoniou, M.; Harman, S.; Ahmad, B.I. Convolutional Neural Networks for Robust Classification of Drones. In Proceedings of the 2022 IEEE Radar Conference (RadarConf22), New York, NY, USA, 21–25 March 2022; pp. 1–6.
19. Dale, H.; Baker, C.; Antoniou, M.; Jahangir, M.; Atkinson, G.; Harman, S. SNR-Dependent Drone Classification Using Convolutional Neural Networks. *IET Radar Sonar Navig.* **2022**, *16*, 22–33. [CrossRef]
20. Kang, K.-B.; Choi, J.-H.; Cho, B.-L.; Lee, J.-S.; Kim, K.-T. Analysis of Micro-Doppler Signatures of Small UAVs Based on Doppler Spectrum. *IEEE Trans. Aerosp. Electron. Syst.* **2021**, *57*, 3252–3267. [CrossRef]
21. Chen, V.C. *The Micro-Doppler Effect in Radar*; Artech House: London, UK; Norwood, MA, USA, 2011; ISBN 9781608070572.
22. Gong, J.; Li, D.; Yan, J.; Hu, H.; Kong, D. Comparison of Radar Signatures from a Hybrid VTOL Fixed-Wing Drone and Quad-Rotor Drone. *Drones* **2022**, *6*, 110. [CrossRef]
23. Gong, J.; Yan, J.; Li, D. Comparison of micro-Doppler signatures registered using RBM of helicopters and WSM of vehicles. *IET Radar Sonar Navig.* **2019**, *13*, 1951–1955. [CrossRef]
24. Chin, C.; Gopalakrishnan, K.; Egorov, M.; Evans, A.; Balakrishnan, H. Efficiency and Fairness in Unmanned Air Traffic Flow Management. *IEEE Trans. Intell. Transp. Syst.* **2021**, *22*, 5939–5951. [CrossRef]

25. Chen, S.; Ma, D.; Yao, Y.; Wang, X.; Li, C. Cooperative Polynomial Guidance Law with Collision Avoidance and Flight Path Angle Coordination. *Aerosp. Sci. Technol.* **2022**, *130*, 107809. [CrossRef]
26. Yu, J.; Dong, X.; Li, Q.; Lu, J.; Ren, Z. Adaptive Practical Optimal Time-Varying Formation Tracking Control for Disturbed High-Order Multi-Agent Systems. *IEEE Trans. Circuits Syst. I Regul. Pap.* **2022**, *69*, 2567–2578. [CrossRef]